The (Ns)2 (Oi)n (n=1,2) defect in Si from a Density Functional Theory perspective

Papadopoulou, K. A., Chroneos, A. & Christopoulos, S-R. G

DOI 10.1016/j.physb.2022.414184
ISSN 0921-4526

Publisher: Elsevier

Physica B 643 (2022) 414184

Contents lists available at ScienceDirect

Physica B: Physics of Condensed Matter

journal homepage: www.elsevier.com/locate/physb

The $(N_s)_2(O_i)_n$ (n=1,2) defect in Si from a Density Functional Theory perspective

Konstantina A. Papadopoulou [a], Alexander Chroneos [b,c], Stavros-Richard G. Christopoulos [a,*]

[a] Faculty of Engineering, Environment and Computing, Coventry University, Priory Street, Coventry, CV1 5FB, United Kingdom
[b] Department of Electrical and Computer Engineering, University of Thessaly, 38221 Volos, Greece
[c] Department of Materials, Imperial College London, London SW7 2BP, United Kingdom

ARTICLE INFO

Keywords:
Silicon
Nitrogen
Oxygen
DFT

ABSTRACT

Nitrogen constitutes a significant defect in silicon (Si) as it can affect its mechanical properties. Substitutional nitrogen defects can be created from interstitial nitrogen defects during cooling of the crystal. In turn, the substitutional nitrogen atoms can form micro-defects in Si, most important of which are the interstitial oxygen atoms since they have an impact on a device's characteristics. In the present paper, we study the structure of the defect clusters in Si consisting of substitutional nitrogen and interstitial oxygen atoms. We find that the most stable structure is the one containing two interstitial oxygen atoms, while the presence of these interstitials results to narrow-gap semiconductors.

1. Introduction

Numerous years of extensive research has been made on the defect processes of group IV semiconductors [1–8]. For example, as also commented in a recent review [9], Kube et al. [10] proposed that the curvature in the Arrhenius plot on self-diffusion in Si (they measure) is associated with two diffusion mechanisms (vacancies and self-interstitials), but later Saltas et al. [11] explained that these experimental results can also be comprehended by a single diffusion mechanism if the non-linear and harmonic behaviour of the isothermal bulk modulus B is considered in the frame of the thermodynamical model, termed $cB\Omega$ model (where c is a constant and Ω the mean volume per atom), in which the Gibbs self-diffusion activation energy g^{act} scales with B [12,13] since $g^{act} = cB\Omega$.

This extensive research continues to attract the interest of the community, because of the aggressive scaling that led to devices with characteristic dimension of a few nanometers and the inherent need to understand the nature of defects under irradiation to improve devices for medical and scientific reasons [14,15].

Nitrogen (N) defects, despite the fact that they exhibit low solubility [16], have been proven to impact silicon's mechanical properties [16,17]. There are numerous experimental and theoretical studies regarding N-doped Si, with the majority of them focusing on the interstitial defect N_i.

Jones et al. [18] showed that, at room temperature, the dimeric N_i - N_i is the one with the largest concentration. This species however, has diffusivity values lower than 10^{-12} cm^2/s [19], thus it is not as mobile as the single N_i which has diffusivity values larger than 1.5×10^{-9} cm^2/s [19]. In addition, the binding energy of N_i - N_i has been shown to be close to 4 eV [20,21].

The energy barrier for diffusion of the N_i - N_i has varied values in literature, ranging from 1.45 eV to 2.8 eV [16,22,23]. The former value, however, is suggested to be an after-effect of existing vacancies or self-interstitials [16].

Furthermore, nitrogen-vacancy (NV) defects in silicon have been of particular interest due to the fact that they can reduce the formation of vacancy clusters during crystal-growth [24,25]. Goss et al. [26] showed that a N_i - N_i - vacancy complex has a binding energy equal to 1.3 eV while the N_i - N_i - divacancy complex has a binding energy equal to 3.4 eV [21].

While N_i - N_i defects are dominant at equilibrium, during cooling down of the crystal they can trap up to three vacancies [26] and create N_s - N_s, N_i - N_s, or (N_s - N_s)V, where now N_s stands for a substitutional nitrogen. From these, N_s - N_s appears to be the most stable [26].

N_s atoms are responsible for the formation of micro-defects in Si [27]. These micro-defects in turn enhance oxygen (O) precipitation and contract the crystal lattice, thus attracting interstitial atoms [27]. From the latter, interstitial oxygen atoms, O_i, are the most important [28] since they can improve device characteristics if they are located in the bulk of Si [28]. In addition, the presence of O in Si results in faster N diffusion [29].

* Corresponding author.
E-mail address: ac0966@coventry.ac.uk (S.-R.G. Christopoulos).

https://doi.org/10.1016/j.physb.2022.414184
Received 6 May 2022; Received in revised form 7 June 2022; Accepted 6 July 2022
Available online 11 July 2022

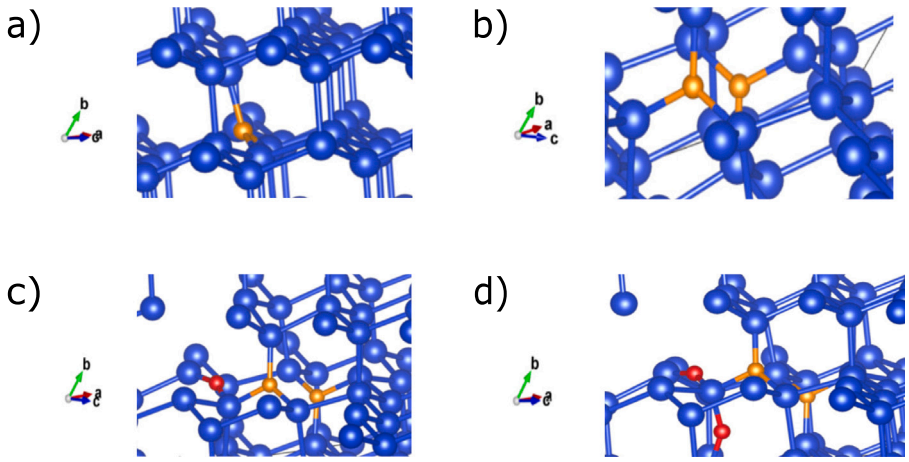

Fig. 1. Zoomed in structures for the (a) N_s, (b) N_s - N_s, (c) $(N_s)_2O_i$ and (d) $(N_s)_2(O_i)_2$ defects in bulk Si. Blue spheres: Si atoms. Brown spheres: N_s atoms. Red spheres: O_i atoms. (For interpretation of the references to colour in this figure legend, the reader is referred to the web version of this article.)

In the present study, we investigate the lowest energy configuration of the $(N_s)_2O_i$ and $(N_s)_2(O_i)_2$ defects using Density Functional Theory (DFT), in order to gain insight into their structure and energetics.

2. Computational methods

The calculations were performed using the plane-wave DFT code as implemented in the CASTEP package [30–34]. To account for the exchange–correlation interactions, we used the generalized gradient approximation (GGA) method and with ultrasoft pseudopotentials [35] to describe the electron-ion interactions [36]. A 250-atoms supercell was used for the bulk Si structure. The cut-off energy was 350 eV and a $2 \times 2 \times 2$ Monkhorst–Pack k-point grid was used [37]. The structures were fully optimized using Broyden–Fletcher–Goldfarb–Shanno (BFGS) geometry optimization method [34,38].

A number of 1000 calculations were executed for each defect until the lowest energy structure was reached. Rather than setting up the calculations by hand, we used the DIMS tool [39] to automate the process of inserting the N_S and O_i defects in bulk Si.

The figures in this paper were produced using the VESTA software [40].

Finally, the binding energies whose minimization helps distinguish between the stablest structure, were calculated using the following formula [41]:

$$E_b = E_{DefectCluster} - \Sigma E_{Isolated\,Defects} \tag{1}$$

Negative E_b implies that a cluster is energetically favourable. Considering Eq. (1), we have for N_s - N_s, $(N_s)_2O_i$, and $(N_s)_2(O_i)_2$, the following equations for the binding energies respectively:

$$\begin{aligned} &E_b(\mathrm{N_sN_sSi}_{N-2}) = \\ &[E(\mathrm{N_sN_sSi}_{N-2}) - E(\mathrm{Si}_N)] - [2E(\mathrm{N_sSi}_{N-1}) - 2E(\mathrm{Si}_N)] = \\ &E(\mathrm{N_sN_sSi}_{N-2}) - 2E(\mathrm{N_sSi}_{N-1}) + E(\mathrm{Si}_N) \end{aligned} \tag{2}$$

where $E(\mathrm{N_sN_sSi}_{N-2})$ is the energy of the N_s - N_s defect in the $N-2$ Si atoms supercell, $E(\mathrm{N_sSi}_{N-1})$ is the energy of the N_s defect in the $N-1$ Si atoms supercell and $E(\mathrm{Si}_N)$ is the energy of the $N = 250$ Si atoms supercell.

$$\begin{aligned} &E_b(\mathrm{N_sN_sO_iSi}_{N-2}) = [E(\mathrm{N_sN_sO_iSi}_{N-2}) - E(\mathrm{Si}_N)] - \\ &[2E(\mathrm{N_sSi}_{N-1}) - 2E(\mathrm{Si}_N)] - [E(\mathrm{O_iSi}_N) - E(\mathrm{Si}_N)] = \\ &E(\mathrm{N_sN_sO_iSi}_{N-2}) - 2E(\mathrm{N_sSi}_{N-1}) - E(\mathrm{O_iSi}_N) + 2E(\mathrm{Si}_N) \end{aligned} \tag{3}$$

where $E(N_sN_sO_iSi_{N-2})$ is the energy of the $(N_s)_2O_i$ defect cluster in the $N-2$ Si atoms supercell and $E(O_i\mathrm{Si}_N)$ is the energy of O_i in the $N = 250$ Si atoms supercell.

$$\begin{aligned} &E_b(\mathrm{N_sN_sO_iO_iSi}_{N-2}) = [E(\mathrm{N_sN_sO_iO_iSi}_{N-2}) - E(\mathrm{Si}_N)] - \\ &[2E(\mathrm{N_sSi}_{N-1}) - 2E(\mathrm{Si}_N)] - [2E(O_i\mathrm{Si}_N) - 2E(\mathrm{Si}_N)] = \\ &E(\mathrm{N_sN_sO_iO_iSi}_{N-2}) - 2E(\mathrm{N_sSi}_{N-1}) - 2E(\mathrm{O_iSi}_N) + \\ &3E(\mathrm{Si}_N) \end{aligned} \tag{4}$$

where $E(\mathrm{N_sN_sO_iO_iSi}_{N-2})$ is the energy of the $(N_s)_2(O_i)_2$ defect cluster in the $N-2$ Si atoms supercell.

3. Results & discussion

We used a step-by-step approach, by first calculating the minimum energy structure of N_s and then the dimer N_s - N_s. Then, we added one, and finally two O_i. As mentioned in Section 2, we explored all possible configurations by placing each O_i in all possible sites in the supercell, that is in a $10 \times 10 \times 10$ grid in a $13.5 \times 13.5 \times 13.5$ Å cube around N_s - N_s for the $(N_s)_2O_i$ cluster and around N_s - N_s - O_i for the $(N_s)_2(O_i)_2$ cluster.

The structures for the N_s, N_s - N_s, $(N_s)_2O_i$ and $(N_s)_2(O_i)_2$ defects are shown in Fig. 1, zoomed in. In Fig. 1c and d in particular, we can see how the existence of interstitial oxygen atoms leads to vacancies in the Si lattice when compared to the cases with N_s, since some breakage in the crystal lattice appears, leaving consecutive Si atoms unbonded.

Regarding a single N_s, it is found that it bonds with three silicon atoms. A simplified version of its bonds with neighbouring Si atoms is shown in Fig. 2. The bond lengths d_1, d_2, d_3 as shown in Fig. 2 are equal to each other (1.86 Å), and much smaller than the average Si-Si bond (2.4 Å). The angles Si - N_s - Si are all equal to 117.64°.

In Fig. 3, we can see the simplified structure of the N_s - N_s defect as well as the calculated bond lengths and angles between the atoms. It is evident that the addition of a second N_s atom slightly decreases the bond lengths between N_s and Si to 1.84 Å on average, while the angles Si - N_s - Si slightly increase to 118°. Each N_s atom is equidistant to all its neighbouring Si atoms, like in the case of a single N_s atom. The inter-silicon distances, however, i.e., the distances between consecutive Si atoms, do not differ from the average Si - Si bond length ([2.3 – 2.4] Å). Therefore, the existence of an extra substitutional nitrogen atom does not seem to affect the bulk silicon bonds.

The simplified structure of the $(N_s)_2O_i$ defect cluster and the calculated bond lengths and angles between the atoms can be seen in Fig. 4. The insertion of an interstitial oxygen atom in the structure, appears to distort the bonds between the second N_s atom (Ns2 in Fig. 4) and its surrounding Si atoms, with a maximum decrease of 2.3% when it comes to the Si atom closest to the O_i atom (Si22 in Fig. 4). However, the existence of the N_s atoms does not appear to affect the O_i - Si bonds, whose length remains equal to those referred in literature ([1.62 – 1.64] Å) [42]. The same behaviour is observed for the inter-silicon bonds, where the O_i does not affect the respective bond lengths or angles.

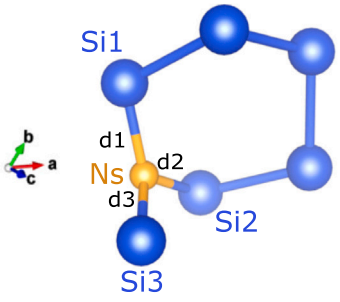

d1=1.86027Å
d2=1.86027Å
d3=1.86030Å

Angles:
Si1-Ns-Si2=117.6368°
Si1-Ns-Si3=117.6368°
Si2-Ns-Si3=117.6367°

Fig. 2. A simplified version of the N_s defect in bulk Si where the calculated bond lengths d1, d2, d3 are also noted.

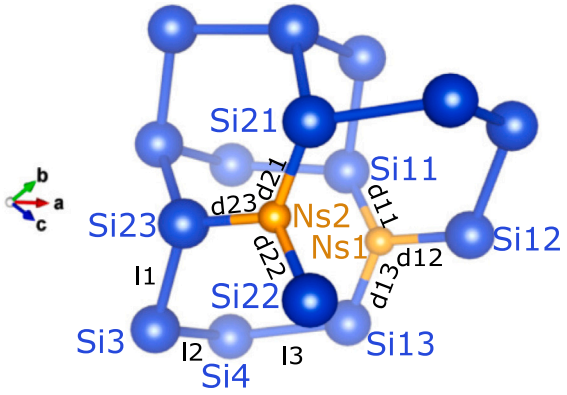

d11=1.83629Å d21=1.83693Å l1=2.42289Å
d12=1.83629Å d22=1.83358Å l2=2.37639Å
d13=1.83570Å d23=1.83535Å l3=2.42299Å

Angles:
Si11-Ns1-Si12=118.0448°
Si11-Ns1-Si13=117.9900°
Si12-Ns1-Si13=118.0679°

Si21-Ns2-Si22=118.0485°
Si21-Ns2-Si23=117.9785°
Si22-Ns2-Si23=118.1013°

Si3-Si4-Si13=110.6252°
Si23-Si3-Si4=110.6875°

Fig. 3. A simplified version of the N_s - N_s defect and the calculated bond lengths and angles between the atoms.

Furthermore, the area around the second N_s atom (which is closest to the O_i atom) has changed drastically, as the orientation of this group of atoms in space has changed significantly. In particular, the angles between the N_s and its bonding Si atoms that previously were all equal to 118° have decreased by 3% (the smallest one) and increased by 4.2% (the largest one). Finally, the area around the first N_s atom (Ns1 in Fig. 4) remains unaffected by the addition of O_i regarding both the bond lengths and the angles between the atoms.

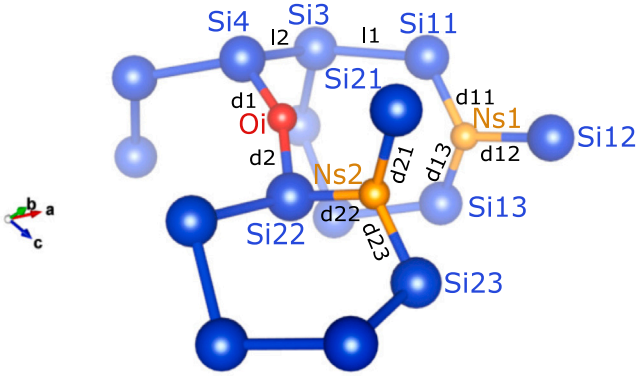

d11=1.84648Å d21=1.84623Å l1=2.44828Å d1=1.64767Å
d12=1.83946Å d22=1.79333Å l2=2.34498Å d2=1.61940Å
d13=1.83592Å d23=1.80766Å

Angles:
Si11-Ns1-Si12=118.3519°
Si11-Ns1-Si13=118.6685°
Si12-Ns1-Si13=116.8472°

Si21-Ns2-Si22=117.3448°
Si21-Ns2-Si23=123.0221°
Si22-Ns2-Si23=114.6128°

Si4-Oi-Si22=153.2459°
Si11-Si3-Si4=110.9490°
Oi-Si22-Ns2=102.2329°
Oi-Si4-Si3=98.7618°

Fig. 4. A simplified version of the $(N_s)_2O_i$ defect cluster and the calculated bond lengths and angles between the atoms.

Table 1
The binding energies for each defect considered.

Defect	E_b (eV)
N_s - N_s	−2.75
$(N_s)_2O_i$	−3.49
$(N_s)_2(O_i)_2$	−4.44

Finally, in Fig. 5, we can see the simplified structure of the $(N_s)_2(O_i)_2$ defect cluster and the calculated bond lengths and angles. The presence of the second O_i atom does not further affect the bond lengths around the first N_s atom (Ns1 in Fig. 5). However, the orientation of that particular sub-cluster changes, with the angles between N_s and the bonding Si atoms differing up to 0.87% from the corresponding ones in the $(N_s)_2O_i$ defect cluster case.

Regarding the sub-cluster around the second N_s atom (Ns2 in Fig. 5), the bond lengths between N_s and the bonding Si atoms show a decrease up to 2.3%. The angles between the aforementioned atoms also appear to be significantly affected by the existence of a second O_i atom. In particular, they have a maximum decrease by 3.2%, while the largest one has increased by 4.9%.

In addition, the second O_i atom does not seem to affect the inter-silicon bonds. However, the O_i - Si bond lengths exhibit a decrease up to 0.98% and an increase up to 0.8% from the minimum and maximum values, respectively, referred in literature ([1.62 – 1.64] Å). Finally, the two O_i atoms are connected through a Si atom, forming an angle of 104.46°.

In Table 1, we can see the binding energies for each defect. It is evident that the most stable form is the full defect cluster $(N_s)_2(O_i)_2$.

In Fig. 6, we can see the calculated Density of States (DOS) for each structure. For the N = 250-atom supercell of bulk Si (Fig. 6a), the

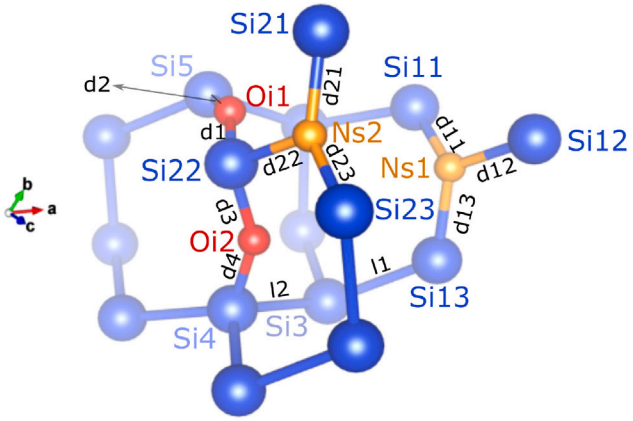

d11=1.84379Å d21=1.81875Å l1=2.44470Å d1=1.60418Å
d12=1.84360Å d22=1.75265Å l2=2.34932Å d2=1.65301Å
d13=1.84630Å d23=1.81741Å d3=1.60421Å
d4=1.65299Å

Angles:
Si11-Ns1-Si12=117.3239°
Si11-Ns1-Si13=119.0259°
Si12-Ns1-Si13=117.6315°

Si21-Ns2-Si22=113.6337°
Si21-Ns2-Si23=129.1044°
Si22-Ns2-Si23=112.9954°

Si4-Si3-Si13=109.0718°
Si22-Oi2-Si4=151.0575°
Si5-Oi1-Si22=152.3624°
Oi1-Si22-Oi2=104.4631°
Oi1-Si22-Ns2=107.8556°
Oi2-Si4-Si3=97.4343°
Oi2-Si22-Ns2=107.3414°
Si3-Si13-Ns1=121.7943°

Fig. 5. A simplified version of the $(N_s)_2(O_i)_2$ defect cluster and the calculated bond lengths and angles between the atoms.

bandgap is calculated at $\backsim 0.6$ eV, indicating that bulk Si is a semiconductor. This value is in agreement with previous studies [43,44] despite the fact that it is almost half of the experimental one which is equal to 1.17 eV [45]. This underestimation is well documented in literature [46,47] and it stems from the use of GGA functionals which contain non-physical self-Coulomb repulsions [48]. In fact, Bagayoko [49] found the bandgap underestimation to be from 30% to 50% using both GGA and LDA (Local Density Approximation) functionals. According to the above, the bandgap in Si can theoretically be as low as 0.585 eV.

Regarding the two N_s atoms, the DOS plot (Fig. 6c) shows that the structure is a semiconductor with smaller bandgap than bulk Si and equal to $\backsim$0.5 eV. The semiconducting behaviour holds true with the addition of first one and then two interstitial oxygen atoms.

4. Summary and concluding remarks

In the present paper, we studied the structure of defect clusters in Si consisting of substitutional nitrogen and interstitial oxygen atoms. We found that the existence of N_s atoms does not affect the bond lengths between consecutive Si atoms.

The insertion of one O_i, which has as favourable site the middle of a Si - Si bond, resulted to a decrease in the bond length between N_s and Si, however the O_i - Si bonds remained unaffected by the existence of N_s. In addition, the second O_i changed the orientation of the defect cluster inside the bulk structure.

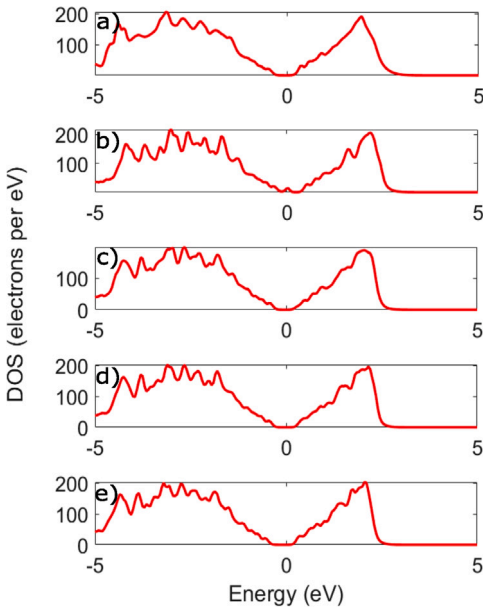

Fig. 6. DOS of (a) $N = 250$-atom supercell of bulk Si, (b) the structure with a N_s defect in the $N-1$ Si atoms supercell, (c) the structure with 2 N_s defects in the $N-2$ Si atoms supercell, (d) the structure with 2 N_s defects and an O_i in the $N-2$ Si atoms supercell and (e) the structure with 2 N_s defects and 2 O_i in the $N-2$ Si atoms supercell. In all cases, the Fermi energy is shifted at 0 eV.

The calculation of the binding energies revealed that the most stable structure is that containing the $(N_s)_2(O_i)_2$ defect cluster. Finally, the DOS analysis showed that while the bulk Si is semiconducting, the structures with O_i appear to be narrow-gap semiconductors.

CRediT authorship contribution statement

Konstantina A. Papadopoulou: Conceptualization, Methodology, Validation, Formal analysis, Investigation, Resources, Data curation, Writing – original draft, Visualization. **Alexander Chroneos:** Conceptualization, Writing – review & editing, Project administration. **Stavros-Richard G. Christopoulos:** Conceptualization, Methodology, Validation, Resources, Data curation, Formal analysis, Writing – review & editing, Supervision, Project administration, Funding acquisition.

Declaration of competing interest

The authors declare that they have no known competing financial interests or personal relationships that could have appeared to influence the work reported in this paper.

Data availability

Data will be made available on request.

Acknowledgements

K. A. Papadopoulou acknowledges support from the International Consortium of Nanotechnologies (ICON) funded by Lloyd's Register Foundation, United Kingdom, a charitable foundation which helps to protect life and property by supporting engineering-related education, public engagement and the application of research.

References

[1] V. Markevich, I. Hawkins, A. Peaker, V. Litvinov, L. Murin, L. Dobaczewski, J. Lindström, Appl. Phys. Lett. 81 (2002) 1821.
[2] H. Silvestri, H. Bracht, J.L. Hansen, A.N. Larsen, E. Haller, Semicond. Sci. Technol. 21 (2006) 758.
[3] K. Kita, S. Suzuki, H. Nomura, T. Takahashi, T. Nishimura, A. Toriumi, Japan. J. Appl. Phys. 47 (2008) 2349.
[4] A. Chroneos, C. Jiang, R. Grimes, U. Schwingenschlögl, H. Bracht, Appl. Phys. Lett. 95 (2009) 112101.
[5] Y. Oshima, M. Shandalov, Y. Sun, P. Pianetta, P.C. McIntyre, Appl. Phys. Lett. 94 (2009) 183102.
[6] H. Wang, A. Chroneos, C. Londos, E. Sgourou, U. Schwingenschlögl, Sci. Rep. 4 (2014) 1.
[7] A. Chroneos, E. Sgourou, C. Londos, U. Schwingenschlögl, Appl. Phys. Rev. 2 (2015) 021306.
[8] H. Nagakura, K. Sueoka, E. Kamiyama, ECS J. Solid State Sci. Technol. 10 (2021) 123003.
[9] P.A. Varotsos, N.V. Sarlis, E.S. Skordas, Crystals 12 (2022) 686.
[10] R. Kube, H. Bracht, E. Hüger, H. Schmidt, J.L. Hansen, A.N. Larsen, J. Ager, E. Haller, T. Geue, J. Stahn, Phys. Rev. B 88 (2013) 085206.
[11] V. Saltas, A. Chroneos, F. Vallianatos, RSC Adv. 6 (2016) 53324.
[12] P. Varotsos, K. Alexopoulos, Phys. Rev. B 22 (1980) 3130.
[13] K. Alexopoulos, P. Varotsos, Phys. Rev. B 24 (1981) 3606.
[14] D. Hall, D. Wood, N. Murray, J. Gow, A. Chroneos, A. Holland, J. Instrum. 12 (2017) P01025.
[15] M. Mamor, K. Bouziane, M. Maaza, J. Appl. Phys. 126 (2019) 235707.
[16] N. Fujita, R. Jones, J. Goss, P. Briddon, T. Frauenheim, S. Öberg, Appl. Phys. Lett. 87 (2005) 021902.
[17] V. Voronkov, R. Falster, Proceedings-Electrochemical Society, Electrochemical Society, 2004, pp. 86–101.
[18] R. Jones, S. Öberg, F.B. Rasmussen, B.B. Nielsen, Phys. Rev. Lett. 72 (1994) 1882.
[19] V.V. Voronkov, R.J. Falster, Solid State Phenomena, Vol. 95, Trans Tech Publ, 2004, pp. 83–92.
[20] H. Sawada, K. Kawakami, Phys. Rev. B 62 (2000) 1851.
[21] H. Kageshima, A. Taguchi, K. Wada, Appl. Phys. Lett. 76 (2000) 3718.
[22] A. Giannattasio, S. Senkader, R. Falster, P. Wilshaw, Physica B 340 (2003) 996.
[23] T. Itoh, T. Abe, Appl. Phys. Lett. 53 (1988) 39.
[24] H. Ishii, S. Shiratake, K. Oka, K. Motonami, T. Koyama, J. Izumitani, Japan. J. Appl. Phys. 35 (1996) L1385.
[25] H. Kageshima, A. Taguchi, K. Wada, MRS Online Proc. Libr. (OPL) 719 (2002).
[26] J. Goss, I. Hahn, R. Jones, P. Briddon, S. Öberg, Phys. Rev. B 67 (2003) 045206.
[27] F. Shimura, R. Hockett, Appl. Phys. Lett. 48 (1986) 224.
[28] G. Kissinger, Defects and Impurities in Silicon Materials, Springer, 2015, pp. 273–341.
[29] A. Gali, J. Miro, P. Deák, C.P. Ewels, R. Jones, J. Phys.: Condens. Matter 8 (1996) 7711.
[30] S.J. Clark, M.D. Segall, C.J. Pickard, P.J. Hasnip, M.I. Probert, K. Refson, M.C. Payne, Z. Kristallogr.-Cryst. Mater. 220 (2005) 567.
[31] P. Hohenberg, W. Kohn, Phys. Rev. 136 (1964) B864.
[32] W. Kohn, L.J. Sham, Phys. Rev. 140 (1965) A1133.
[33] M.C. Payne, M.P. Teter, D.C. Allan, T. Arias, J.D. Joannopoulos, Rev. Modern Phys. 64 (1992) 1045.
[34] B.G. Pfrommer, M. Cote, S.G. Louie, M.L. Cohen, J. Comput. Phys. 131 (1997) 233.
[35] D. Vanderbilt, Phys. Rev. B 41 (1990) 7892.
[36] W. Wan, H. Wang, Materials 8 (2015) 6163.
[37] H.J. Monkhorst, J.D. Pack, Phys. Rev. B 13 (1976) 5188.
[38] D. Packwood, J. Kermode, L. Mones, N. Bernstein, J. Woolley, N. Gould, C. Ortner, G. Csányi, J. Chem. Phys. 144 (2016) 164109.
[39] S.-R.G. Christopoulos, K.A. Papadopoulou, A. Konios, D. Parfitt, Comput. Mater. Sci. 202 (2022) 110976.
[40] K. Momma, F. Izumi, J. Appl. Crystallogr. 44 (2011) 1272.
[41] S.-R. Christopoulos, H. Wang, A. Chroneos, C.A. Londos, E.N. Sgourou, U. Schwingenschlögl, J. Mater. Sci., Mater. Electron. 26 (2015) 1568.
[42] H. Chen, S. Adams, IUCrJ 4 (2017) 614.
[43] Z.-h. Yang, H. Peng, J. Sun, J.P. Perdew, Phys. Rev. B 93 (2016) 205205.
[44] M. Potsidi, N. Kuganathan, S.-R. Christopoulos, N. Sarlis, A. Chroneos, C. Londos, AIP Adv. 12 (2022) 025112.
[45] W. Bludau, A. Onton, W. Heinke, J. Appl. Phys. 45 (1974) 1846.
[46] J.M. Crowley, J. Tahir-Kheli, III. W. A. Goddard, J. Phys. Chem. Lett. 7 (2016) 1198.
[47] J.P. Perdew, W. Yang, K. Burke, Z. Yang, E.K. Gross, M. Scheffler, G.E. Scuseria, T.M. Henderson, I.Y. Zhang, A. Ruzsinszky, et al., Proc. Natl. Acad. Sci. 114 (2017) 2801.
[48] J.P. Perdew, A. Zunger, Phys. Rev. B 23 (1981) 5048.
[49] D. Bagayoko, AIP Adv. 4 (2014) 127104.